European Journal of Radiology 82 (2013) 1552–1557

Contents lists available at SciVerse ScienceDirect

European Journal of Radiology

journal homepage: www.elsevier.com/locate/ejrad

Altered regional homogeneity patterns in adults with attention-deficit hyperactivity disorder

Xunheng Wang[a,c], Yun Jiao[b,*], Tianyu Tang[a,c], Hui Wang[a,c], Zuhong Lu[a,c]

[a] School of Biological Science and Medical Engineering, Southeast University, Nanjing 210096, China
[b] Jiangsu Key Laboratory of Molecular Imaging and Functional Imaging, Department of Radiology, Zhongda Hospital, Medical School of Southeast University, Nanjing 210009, China
[c] Key Laboratory of Child Development and Learning Science (Ministry of Education), Southeast University, Nanjing 210096, China

ARTICLE INFO

Article history:
Received 23 January 2013
Accepted 17 April 2013

Keywords:
Resting state fMRI
ADHD
Discriminative model
Regional homogeneity

ABSTRACT

Purpose: Investigating the discriminative brain map for patients with attention-deficit/hyperactivity disorder (ADHD) based on feature selection and classifier; and identifying patients with ADHD based on the discriminative model.

Materials and methods: A dataset of resting state fMRI contains 23 patients with ADHD and 23 healthy subjects were analyzed. Regional homogeneity (ReHo) was extracted from resting state fMRI signals and used as model inputs. Raw ReHo features were ranked and selected in a loop according to their p values. Selected features were trained and tested by support vector machines (SVM) in a cross validation procedure. Cross validation was repeated in feature selection loop to produce optimized model.

Results: Optimized discriminative map indicated that the ADHD brains exhibit more increased activities than normal controls in bilateral occipital lobes and left front lobe. The altered brain regions included portions of basal ganglia, insula, precuneus, anterior cingulate cortex (ACC), posterior cingulate cortex (PCC), thalamus, and cerebellum. Correlation coefficients indicated significant positive correlation of inattentive scores with bilateral cuneus and precuneus, and significant negative correlation of hyperactive/impulsive scores with bilateral insula and claustrum. Additionally, the optimized model produced total accuracy of 80% and sensitivity of 87%.

Conclusion: ADHD brain regions were more activated than normal controls during resting state. Linear support vector classifier can provide useful discriminative information of altered ReHo patterns for ADHD; and feature selection can improve the performances of classification.

1. Introduction

Attention-deficit/hyperactivity disorder (ADHD), defined as age-inappropriate levels of hyperactivity, impulsivity and inattention evaluated by Diagnostic and Statistical Manual of Mental Disorders (DSM IV) [1], is a developmental disorder that starts at childhood and persists into adulthood in behavioral and cognitive phenotype [2]. Nearly 5–10% of school aged children and 4% of adults in the USA suffer from ADHD [3]. Structural magnetic resonance imaging (MRI) indicated the abnormalities of ADHD with methods of both voxel based morphometry [4] and thickness based morphometry [5]. Dorsolateral prefrontal cortex, anterior cingulate cortex, putamen, inferior parietal lobule, cerebellum and brain regions that consist of attention and execution networks were reported for statistics difference by morphometry [4,5]. Diffusion tensor imaging found the abnormalities in left inferior longitudinal fasciculus, cingulum bundle, corpus callosum, right premotor, left cerebellum, internal capsule, basal ganglia, thalamus, etc. [6–8].

Resting state fMRI has attracted a significant amount of interests recently. Slow fluctuations of BLOD signals were found in human brain with absence of goal-directed tasks and external input recorded by fMRI [9]. Regional homogeneity (ReHo) was widely applied for resting state fMRI research [10,11]. ReHo measures the regional similarity of brain activity during fMRI [12]. Current resting state fMRI studies found abnormalities of ADHD in sensorimotor cortex, cerebellum, anterior cingulated cortex (ACC), brainstem, default mode network and other related brain regions [12–14].

In addition to the extensive researches on abnormalities of ADHD with brain morphometry and connectivity, the interests of discriminative models for ADHD have been promoted by the ADHD-200 consortium [15] and 1000 Functional Connectomes Project. Discriminative models for ADHD can provide diagnostic information for each subject and evaluate the discriminative power of brain voxels, which is more helpful than statistics analysis methods on

* Corresponding author. Tel.: +86 25 8327 2541; fax: +86 25 8327 2541.
E-mail address: yunjiao@seu.edu.cn (Y. Jiao).

0720-048X/$ – see front matter © 2013 Elsevier Ireland Ltd. All rights reserved.
http://dx.doi.org/10.1016/j.ejrad.2013.04.009

Table 1
Subjects' demographic variables.

	ADHD	VC	*p*-Value
Number of subjects	23	23	–
Gender (male:female)	18:5	18:5	1
Age (year)	35.14 ± 9.75	32.04 ± 9.23	0.28
Inattentive	17 ± 4.97	–	–
Hyperactive/impulsive	13 ± 5.28	–	–

group-level [16,17]. Discriminative models are based on pattern classification techniques. In a previous study, four classifiers were successfully applied to build predictive models for children with autism spectral disorder (ASD) [18]. Several research groups had also applied classification method for diagnosis of other neuro-related disease or disorder, such as Alzheimer's disease [19] and very mild dementia [20]. Specially, a previous study about ADHD attempted to classify ADHD using fisher discriminative analysis, and obtained total accuracy of 85% and sensitivity of 78% from only 20 samples (9 patients vs 11 normal controls) [16]. In addition, their model was indirect and difficult to interpret due to principle component analysis, a feature extraction method. Generally, feature processing includes two parts, feature extraction and feature selection [21]. However, to our knowledge, few studies focused on investigating the contribution of feature selection for producing discriminative map for ADHD.

Based on current studies, we hypothesized that the patients with ADHD would possess characteristic ReHo patterns which can be discovered by feature selection. To test this hypothesis, we used resting state fMRI to construct ReHo map of both ADHD patients and normal controls. Firstly, a simple *t*-test was applied to rank ReHo features of gray matter. Secondly, features with *p* values in ascending order were selected in a loop. Thirdly, the selected features were taken as inputs for support vector classifier. Finally, an optimized discriminative map of ReHo for ADHD was created based on the accuracy curves of feature selection loop.

2. Method

2.1. Participants

All resting state fMRI images and structural MRI images were downloaded from the 1000 Functional Connectomes Project (http://www.nitrc.org/projects/fcon_1000/). The data-release is unrestricted for researchers to publish with any part of the dataset. The subjects used in this study were age and gender matched, including 23 ADHD participants (18 males; mean age 35.14 ± 9.75) and 23 healthy participants (18 males; mean age 32.04 ± 9.23). All patients met lifetime criteria for Combined Type ADHD [14]. All participants provided signed informed consent as approved by the institutional review boards of NYU and the NYU School of Medicine [14]. The demographics information is presented in Table 1. Because ADHD rating scale (ADHD-RS) assessments [22] were only performed in the ADHD group, we could not obtain the ADHD-RS statistics for the normal group.

2.2. Imaging methods

Resting-state fMRI data were acquired on a Siemens Allegra 3.0 Tesla scanner. For each participant, resting-state fMRI images scan was consisted of 192 continuous EPI functional volumes (TR = 2000 ms; TE = 25 ms; flip angle = 90, 39 slices, matrix = 64 × 64; FOV = 192 mm; acquisition voxel size = 3 mm × 3 mm × 3 mm) and a high-resolution T1-weighted volume using magnetization prepared gradient echo sequence (TR = 2500 ms; TE = 4.35 ms; T1 = 900 ms; flip angle = 8; 176 slices, FOV = 256 mm). All participants were instructed to remain relax with their eyes open during each scan while the word "Relax" was centrally displayed [14].

2.3. Data preprocessing

Structural MRI data were segmented and linear normalized to MNI standard brain space. Resting-state fMRI data were preprocessed by the following steps: (1) discard the first 4 volumes; (2) slice timing; (3) motion correction; (4) co-register functional volumes to MNI standard brain space with spatial resolution of 4 mm × 4 mm × 4 mm; (5) regress out nuisances as well as a low order polynomial (detrending); (6) temporally band-pass filtering (0.009–0.08 Hz); (7) blur the filtered data with a 6 mm FWHM Gaussian kernel. Head motions for all subjects were within 3 mm translation and 3 degree rotation. The whole preprocessing steps were built in a script according to Athena Pipeline from the NeuroBureau (http://neurobureau.projects.nitrc.org) with AFNI (afni.nimh.nih.gov/afni) and FSL 4.1.9 (www.fmrib.ox.ac.uk/fsl/) [14].

2.4. Regional homogeneity

Regional homogeneity (ReHo) was widely used for resting fMRI study [16,23]. ReHo is a voxel-wise parameter which measures the similarity of a given voxel with its nearest neighbors by resting state fMRI. ReHo is based on the theory that voxels within a functional brain region show greater temporally homogeneity when that area is activated during rest or task conditions [16]. Kendall's coefficient concordance is used to calculate ReHo value at each voxel with time courses in its neighborhood cluster [23]. The ReHo value of a voxel indicates the degree of regionally temporal synchronization within the neighborhood cluster [16].

2.5. Leave one out cross validation

To create the finale ReHo map with the highest discriminative power, leave-one-out cross-validation (LOOCV) was applied [11,16]. LOOCV takes one instance from the original sample as the validation data, and leaves the remained observations as the training data. This procedure was repeated 46 times so that each instance of the 46 subjects was used once as the validation data. LOOCV is the same as a *K*-fold cross-validation with *K* being equal to the total number of all instances. In this paper, *K* equals to 46.

2.6. Feature selection

In this study, ReHo of gray matter was investigated as raw features using anatomical automatic labeling (AAL) template as mask. The masked ReHo features were selected and invalidated in LOOCV. For each fold of LOOCV, feature selection was applied on training sets. ReHo features for gray matter were extracted and ranked by simple *t*-test. The order of the rearranged features was sorted in an ascending way. Ranked features were selected in a loop with increase length of 100. For each step of the loop, the selected features were taken as inputs for support vector classifier. The number of input features started from 100 to 8000, and produced the curves of accuracy with 80 points for each step of feature selection. It should be noted that the feature ranking and selection methods were built in the nested LOOCV procedure. The feature selection method is illustrated in Fig. 1.

2.7. Sequential minimal optimization

Sequential minimal optimization (SMO) was applied to train and test the selected features. SMO is a fast iterative algorithm

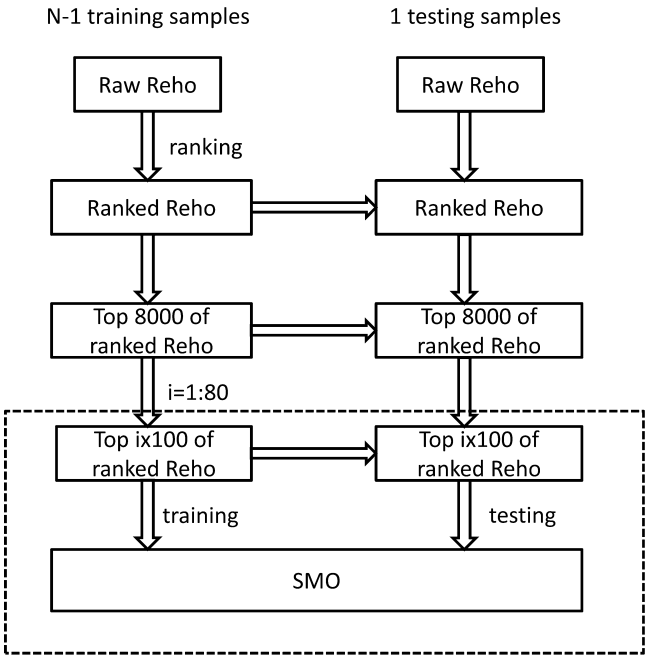

Fig. 1. Feature selection in each fold of LOOCV. The dotted box repeated 80 times in order to find the optimum accuracy of classification.

to efficiently solve the optimization problem in support vector machines (SVMs). It divides the optimization problem of SVMs into a set of smallest possible sub-problems, which are then solved analytically [10]. SMO significantly improves scaling and computation time of SVMs. SMO is most effective for linear SVMs. The SMO algorithm is slower for non-linear SVMs than linear SVMs, since the computation time is dominated by the evaluation of the SVMs [10]. Here, we used SMO with linear kernel implemented in WEKA (http://www.cs.waikato.ac.nz/ml/weka/), a widely used machine-learning software package [10,18]. The attribute weights w, describe the separating hyperplane of a linear SMO [11]. Parameter w of SMO indicated the contribution of the feature to support vector machines [11]. In this paper, positive w means increased activities in ADHD brains, while negative value means decreased activities [11]. The w map of the optimized features was extracted and projected to brain surface as part of our results. Histogram of w was also reported to show the probability distribution of the attributes.

2.8. Performance of SMO

We evaluated the performance of SMO-based classification by the following metrics: accuracy, sensitivity and specificity. Accuracy is the proportion of correctly labeled instances. Sensitivity is the proportion of positive instances that were correctly reported as being positive. Specificity is the proportion of negative instances that were correctly reported as being negative [18].

3. Results

The curves of accuracy, sensitivity and specificity of ReHo-based classification are shown in Fig. 2. The horizontal axis was the number of selected features with ascending p values. We found that accuracy was continually higher than 80% from top 6100 to 6800. The top 6500 features were selected to generate optimized discriminative map. The optimized accuracy, sensitivity and specificity at the point of top 6500 features were 80%, 87% and 74% respectively.

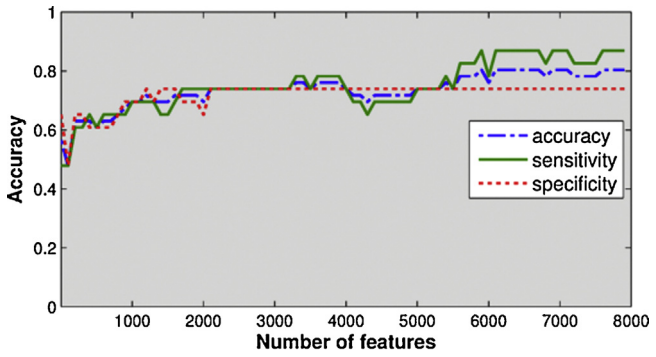

Fig. 2. Performance for ReHo-based classification. Accuracy, sensitivity and specificity curves for feature selection loop were labeled with different colors.

Several clusters of altered ReHo features are found in Fig. 3. Distribution of attribute weights produced by SMO is presented in Fig. 4. Most of the increased regions were located on left hemisphere, while decreased on right: the bilateral occipital lobes and left front lobe exhibited increased activity; while the right front lobe and parietal lobes showed decreased activity. The detailed locations of brain regions and Brodmann Areas (BA) of each cluster are reported in Table 2. Anatomical name of altered brain regions are reported in Table S3 of Supporting Information. The altered brain regions contained portions of basal ganglia, insula, precuneus, anterior cingulate cortex (ACC), posterior cingulate cortex (PCC), thalamus, and cerebellum.

4. Discussion

In this paper, we applied feature selection method to search the optimized discriminative map for ADHD. Our method produced total accuracy of 80% and sensitivity of 87%. To our knowledge, this was the first attempt to use p value as a ranker with fixed step length in a loop for feature selection, and generate optimized discriminative map of ReHo using SMO in Weka. Our model demonstrated that ReHo-SMO based on feature selection had discriminative power to discover the abnormal patterns of ADHD. We found that feature selection with p as ranker was an effective method for classification of ADHD based on ReHo. The sensitivity of 87% is satisfactory for diagnosis. Totally 6 normal controls were mislabeled. The specificity of 74% might be caused by aging of the control group

Table 2
Clusters of most discriminative ReHo features for ADHD subjects.[a]

Cluster	L/R[b]	BA[c]	MNI (x, y, z)[d]	K[e]	Peak w[f]
1	R	4, 6, 7, 13, 40	(64, 4, 38)	335	−0.0083
2	R	9, 10, 46	(40, 64, 10)	189	−0.0116
3	L	3, 4, 5, 7	(−24, −28, 70)	148	−0.0058
4	L	4, 6, 13	(−60, 0, 34)	82	−0.006
5	R	–	(16, 8, 2)	69	−0.0052
6	L/R	6, 8, 9, 10, 46, 47	(−64, −8, 38)	989	0.0116
7	L	7, 17, 18, 19, 31	(−72, −40, 10)	645	0.0153
8	R	18, 19, 20,39	(40, −28, −34)	511	0.0148
9	L	3, 4, 6	(−8, −16, 82)	151	0.0117
10	L/R	–	(−20, −68, −18)	150	0.0057
11	L	20, 21	(−68, −20, −14)	96	0.0091
12	R	13, 22, 41	(44, −8, 30)	89	0.0075
13	R	18, 37, 39	(64, −64, 6)	55	0.0172
14	R	8, 9	(32, 20, 34)	52	0.0049

[a] Reported by FSL's cluster and atlasquery commands.
[b] Left or right cerebral hemisphere.
[c] Brodmann Areas.
[d] Coordinates for the peak voxel.
[e] Voxel number of each cluster.
[f] Attribute weight for the peak voxel.

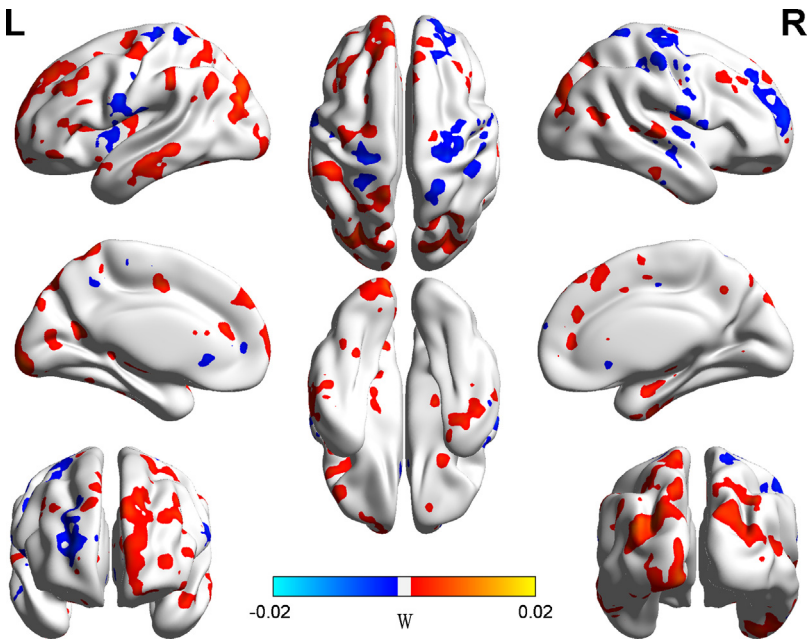

Fig. 3. Optimized discriminative map of ReHo for ADHD patients. The map was composed of the attribute weights *w* of the top 6500 features. Positive *w* with red color means increased ReHo in ADHD brains. Negative *w* with blue color means decreased ReHo value in ADHD brains. The size of each cluster was over 50 voxels. (Discriminative map was demonstrated with the BrainNet Viewer, http://www.nitrc.org/projects/bnv/.)

according to current report of decreased activity in elder brains [24].

From Fig. 4, we found that most discriminative powers were distributed around ± 5‰. The histogram suggested that most of the selected features contributed equally to SMO classifier. The total number of red bars in Fig. 4 indicates that ADHD brains are more activated than normal controls. The results were consistent with current report that ADHD patients exhibited more activities in sensory-related cortex during resting state [25].

The advantage of linear support vector machines is that it can provide functional neuro-markers for subsequent investigation. Current studies found abnormal regions including cingulate, precuneus, basal ganglia, insula, anterior cingulate cortex (ACC), thalamus and cerebellum in ADHD [7,9,14,16]. Those brain regions were also detected by our feature selection method and SMO. The abnormalities of those regions were reported as follows.

The dysfunction of cingulate–precuneus interactions was reported in ADHD [14]. We found similar results: the decreased ReHo of posterior cingulate and precuneus in clusters 7 and 8 from Table 2 were consistent with decreases in connectivity between precuneus and ventromedial prefrontal cortex and portions of posterior cingulate [14]. Decreased ReHo in anterior and posterior default mode components may suggest the dysfunction for working-memory deficits, while the abnormalities in fronto-default mode interactions of ADHD implicated the lapses of attention [14].

The basal ganglia are associated with a variety of key functions, especially for motor function [26]. Decreased basal ganglia volumes were found in boys with ADHD [27]. This may be the anatomical reason of the abnormal brain function of ADHD found as portions of clusters 5, 6 and 8 from Table 2.

The altered anterior cingulate gyrus and anterior insula which is part of saliency network [28], found as portions of clusters 1, 4, 8

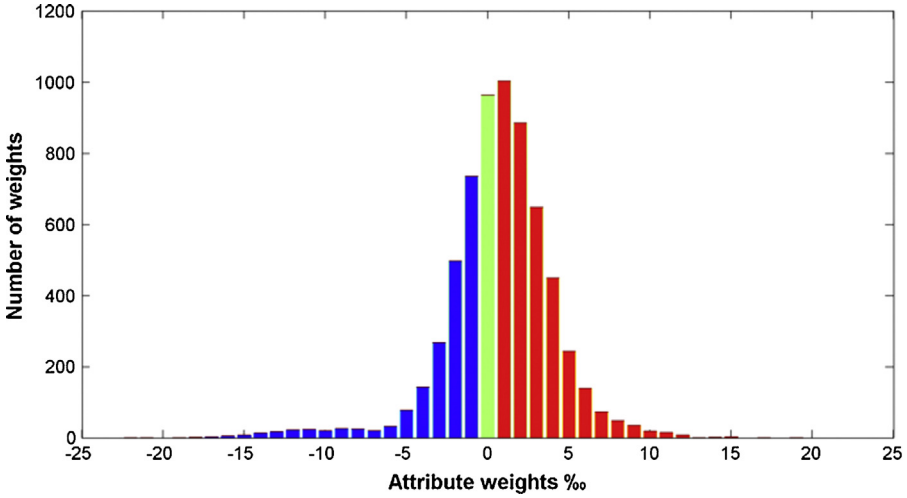

Fig. 4. Histogram for attribute weights of optimized features produced by SMO. Attribute weight is the *w* value at each voxel of the top 6500 features. Color bar in red means increased ReHo in ADHD brains. Color bar in blue means decreased ReHo value in ADHD brains.

and 12 from Table 2, may be involved attentional impairment and distractibility of ADHD. The bilateral thalamus showed increased activity based on cluster 6 from Table 2, which was also found in ADHD [16]. It was reported that the thalamus was an important bridge between the basal ganglia and cerebral cortex. The fronto-striatal circuitry is partly mediated via the thalamus during attention tasks [8]. Decreased fiber tracts connectivity between thalamus and striatum, hippocampus, and prefrontal lobe have been reported in [8]. The cerebellum showed increased activity based on cluster 10 from Table 2, which might be caused by smaller cerebellar volumes in ADHD than normal controls [29].

We also investigated the correlation coefficient map between the ADHD-RS scores and the selected most discriminative ReHo features. The details were reported in Tables S1–S2 and Figures S1–S2 of Supporting Information. Inattentive scores exhibited positive correlation with ReHo, while hyperactive/impulsive scores showed negative correlation with ReHo (Table S1 and Figure S1). We found significant positive correlation of inattentive scores with bilateral cuneus and precuneus, perhaps because inattentive symptoms were highly correlated with ADHD [14]. We found significant negative correlation of hyperactive/impulsive scores with bilateral insula and claustrum (Table S2 and Figure S2). This supported that the working memory and sensorimotor integration of ADHD might be associated with hyperactivity [30].

One limitation of our research was that the LOOCV procedure was performed on small sample size. ADHD-200 consortium provides hundreds of ADHD samples and normal controls to the neuro-imaging community [15]. However, the total accuracy of classification for ADHD-200 was low. The diverse results of current classifications of ADHD might be caused by either population or parameters and image signals on different scanners. In addition, most of these methods did not consider the factor of age and gender. Another limitation is that feature selection did not consider the adjacency and connectivity within whole brain voxels. The brain regions that were not displayed might still be useful for discriminative analysis of ADHD with other classifiers. It should be noted that the sub-types of ADHD were not considered as a factor due to the limitation of demographic data released in this study.

One advantage of our method was that feature selection was embedded in a nested cross validation, the estimated accuracy of which was unbiased and reliable [11,16]. Our results were based on subjects that were age and gender matched, thus the final discriminative map was more representative. For further study, ADHD-200 datasets will be recruited to classification. Sub-types of ADHD, IQ and clinical scores will also be considered with improved feature selection methods and other classifiers.

5. Conclusion

We applied feature selection and support vector machines to classify ADHD patients from normal controls based on voxel-wise ReHo. The experimental results demonstrated that our model possesses discriminative power to discover the abnormal patterns of ADHD.

Conflicts of interest

All authors have no conflicts of interest.

Acknowledgments

This work was supported by National Program on Key Basic Research Project (Nos. 2013CB733800, 2013CB733803) and National Natural Science Foundation of China General Projects (No. 81271739). We thank the 1000 Functional Connectomes Project for sharing the datasets of structural MRI and resting state fMRI.

Appendix A. Supplementary data

Supplementary data associated with this article can be found, in the online version, at http://dx.doi.org/10.1016/j.ejrad.2013.04.009.

References

[1] APA. Diagnostic and statistical manual of mental disorders: DSM-IV-TR. 4th ed. Washington DC: Springer; 2000. p. 943.
[2] Cubillo A, Rubia K. Structural and functional brain imaging in adult attention-deficit/hyperactivity disorder. Expert Review of Neurotherapeutics 2010;10:603–20.
[3] Biederman J. Attention-deficit/hyperactivity disorder: a selective overview. Biological Psychiatry 2005;57:1215–20.
[4] Seidman LJ, Biederman J, Liang L, et al. Gray matter alterations in adults with attention-deficit/hyperactivity disorder identified by voxel based morphometry. Biological Psychiatry 2011;69:857–66.
[5] Makris N, Biederman J, Valera EM, et al. Cortical thinning of the attention and executive function networks in adults with attention-deficit/hyperactivity disorder. Cerebral Cortex (New York, NY: 1991) 2007;17:1364–75.
[6] Ashtari M, Kumra S, Bhaskar SL, et al. Attention-deficit/hyperactivity disorder: a preliminary diffusion tensor imaging study. Biological Psychiatry 2005;57:448–55.
[7] Konrad A, Dielentheis TF, Masri DE, et al. White matter abnormalities and their impact on attentional performance in adult attention-deficit/hyperactivity disorder. European Archives of Psychiatry and Clinical Neuroscience 2012;262:351–60.
[8] Xia S, Li X, Kimball AE, Kelly MS, Lesser I, Branch C. Thalamic shape and connectivity abnormalities in children with attention deficit/hyperactivity disorder. Psychiatry Research: Neuroimaging 2012:1–7.
[9] Biswal BB. Resting state fMRI: a personal history. NeuroImage 2012;62:938–44.
[10] Platt JC. Fast training of support vector machines using sequential minimal optimization. Advances in Kernel methods. MIT Press; 1999. p. 185–208.
[11] Ecker C, Rocha-Rego V, Johnston P, et al. Investigating the predictive value of whole-brain structural MR scans in autism: a pattern classification approach. NeuroImage 2010;49:44–56.
[12] Zang Y-F, He Y, Zhu C-Z, et al. Altered baseline brain activity in children with ADHD revealed by resting-state functional MRI. Brain & Development 2007;29:83–91.
[13] Uddin LQ, Kelly A.M.C., Biswal BB, et al. Network homogeneity reveals decreased integrity of default-mode network in ADHD. Journal of Neuroscience Methods 2008;169:249–54.
[14] Castellanos FX, Margulies DS, Kelly C, et al. Cingulate-precuneus interactions: a new locus of dysfunction in adult attention-deficit/hyperactivity disorder. Biological Psychiatry 2008;63:332–7.
[15] Milham M, Fair D. The ADHD-200 consortium: a model to advance the translational potential of neuroimaging in clinical neuroscience. Frontiers in Systems Neuroscience 2012;6:1–5.
[16] Zhu C-Z, Zang Y-F, Cao Q-J, et al. Fisher discriminative analysis of resting-state brain function for attention-deficit/hyperactivity disorder. NeuroImage 2008;40:110–20.
[17] Craddock RC, Holtzheimer PE, Hu XP, Mayberg HS. Disease state prediction from resting state functional connectivity. Magnetic Resonance in Medicine 2009;62:1619–28.
[18] Jiao Y, Chen R, Ke X, Chu K, Lu Z, Herskovits EH. Predictive models of autism spectrum disorder based on brain regional cortical thickness. NeuroImage 2010;50:589–99.
[19] Cuingnet R, Gerardin E, Tessieras J, et al. Automatic classification of patients with Alzheimer's disease from structural MRI: a comparison of ten methods using the ADNI database. NeuroImage 2011;56:766–81.
[20] Chen R, Herskovits EH. Machine-learning techniques for building a diagnostic model for very mild dementia. NeuroImage 2010;52:234–44.
[21] Liu H, Motoda H. Feature extraction, construction and selection: a data mining perspective Boston, USA: Kluwer Academic Publishers; 1998. p. 438.
[22] Kessler RC, Ph D, Adler L, et al. The prevalence and correlates of adult ADHD in the United States: results from the national comorbidity survey replication. The American Journal of Psychiatry 2006;163:716–23.
[23] Zang Y, Jiang T, Lu Y, He Y, Tian L. Regional homogeneity approach to fMRI data analysis. NeuroImage 2004;22:394–400.
[24] Damoiseaux JS, Beckmann CF, Arigita EJ, et al. Reduced resting-state brain activity in the "default network" in normal aging. Cerebral Cortex 2008;18:1856–64.
[25] Tian L, Jiang T, Liang M, et al. Enhanced resting-state brain activities in ADHD patients: a fMRI study. Brain & Development 2008;30:342–8.
[26] Cao X, Cao Q, Long X, et al. Abnormal resting-state functional connectivity patterns of the putamen in medication-naïve children with attention deficit hyperactivity disorder. Brain Research 2009;1303:195–206.

[27] Qiu A, Crocetti D, Adler M, et al. Basal ganglia volume and shape in children with attention deficit hyperactivity disorder. The American Journal of Psychiatry 2009;166:74–82.
[28] Palaniyappan L, Liddle PF. Does the salience network play a cardinal role in psychosis? An emerging hypothesis of insular dysfunction. Journal of Psychiatry & Neuroscience 2012;37:17–27.
[29] Mackie S, Shaw P, Lenroot R, et al. Cerebellar development and clinical outcome in attention deficit hyperactivity disorder. The American Journal of Psychiatry 2007;164:647–55.
[30] Fassbender C, Schweitzer JB, Cortes CR, et al. Working memory in attention deficit/hyperactivity disorder is characterized by a lack of specialization of brain function. PLoS One 2011;6:e27240.